

International Collaboration Activities on Engineered Barrier Systems

Fuel Cycle Research & Development

*Prepared for
U.S. Department of Energy
Used Fuel Disposition*

**Carlos F. Jove-Colon
Sandia National Laboratories**

August 2016

**FCRD-UFD-2016-000628
SAND2016-XXXXX**



DISCLAIMER

This information was prepared as an account of work sponsored by an agency of the U.S. Government. Neither the U.S. Government nor any agency thereof, nor any of their employees, makes any warranty, expressed or implied, or assumes any legal liability or responsibility for the accuracy, completeness, or usefulness, of any information, apparatus, product, or process disclosed, or represents that its use would not infringe privately owned rights. Reference herein to any specific commercial product, process, or service by trade name, trade mark, manufacturer, or otherwise, does not necessarily constitute or imply its endorsement, recommendation, or favoring by the U.S. Government or any agency thereof. The views and opinions of authors expressed herein do not necessarily state or reflect those of the U.S. Government or any agency thereof.

FCT DOCUMENT COVER SHEET¹

Name/Title of Deliverable/Milestone/Revision No. International Collaboration Activities on Engineered Barrier Systems
M4FT-16SN080302081

Work Package Title and Number DR Argillite Disposal International R&D, FT-16SN08030208

Work Package WBS Number 1.02.08.03.02

Responsible Work Package Manager Jove-Colon, Carlos
(Name/Signature)

Date Submitted

Quality Rigor Level for Deliverable/Milestone ²	<input checked="" type="checkbox"/> QRL-3	<input type="checkbox"/> QRL-2	<input type="checkbox"/> QRL-1 Nuclear Data	<input type="checkbox"/> Lab/Participant QA Program (no additional FCT QA requirements)
--	---	--------------------------------	--	--

This deliverable was prepared in accordance with

Sandia National Laboratories

QA program which meets the requirements of

 DOE Order 414.1 NQA-1-2000 Other**This Deliverable was subjected to:** Technical Review Peer Review**Technical Review (TR)****Peer Review (PR)****Review Documentation Provided****Review Documentation Provided** Signed TR Report or, Signed PR Report or, Signed TR Concurrence Sheet or, Signed PR Concurrence Sheet or, Signature of TR Reviewer(s) below Signature of PR Reviewer(s) below**Name and Signature of Reviewers**

NOTE 1: Appendix E should be filled out and submitted with the deliverable. Or, if the PICS:NE system permits, completely enter all applicable information in the PICS:NE Deliverable Form. The requirement is to ensure that all applicable information is entered either in the PICS:NE system or by using the FCT Document Cover Sheet.

NOTE 2: In some cases there may be a milestone where an item is being fabricated, maintenance is being performed on a facility, or a document is being issued through a formal document control process where it specifically calls out a formal review of the document. In these cases, documentation (e.g., inspection report, maintenance request, work planning package documentation or the documented review of the issued document through the document control process) of the completion of the activity, along with the Document Cover Sheet, is sufficient to demonstrate achieving the milestone. If QRL 1, 2, or 3 is not assigned, then the Lab / Participant QA Program (no additional FCT QA requirements) box must be checked, and the work is understood to be performed and any deliverable developed in conformance with the respective National Laboratory / Participant, DOE or NNSA-approved QA Program.

ACKNOWLEDGEMENTS

The author acknowledges our gratitude to Carlos Miguel Lopez (SNL), Ed Matteo (SNL), Jason Heath (SNL), William Spezialetti (DOE NE-53), Prasad Nair (DOE NE-53), Mark Tynan (DOE NE-53), and Tim Gunther (DOE NE-53) for their helpful discussions and contributions on various topics covered in this report. John Eric Bower (SNL) of the Microsystems Integration Department X-ray performed the CT imaging on the shotcrete-bentonite samples. Mark Rodriguez (SNL), Marshall Reviere (SNL), and James Griego (SNL) conducted the micron-XRF analyses in this study. The assistance of Patrick D. Burton (SNL) with the SEM/EDS system is also appreciated.

This page is intentionally blank.

Table of Contents

Table of Contents.....	vi
Acronym List	viii
I. Introduction	9
II. X-Ray CT Imaging of FEBEX-DP Samples: Shotcrete-Bentonite Interface	11
III. SEM/EDS and Micro-XRF Analysis of FEBEX-DP Samples.....	16
III. DECOVALEX-2019 Task C: GREET (Groundwater REcovery Experiment in Tunnel), Mizunami URL, Japan.....	19
III. Conclusions	24
IV. FY17 Work.....	24
VIII. References	25

Table of Figures

Figure 1. Schematic layout of the FEBEX “in-situ” field test after the first partial dismantling showing the configuration of heater #2 at the GTS URL (García-Siñeriz et al., 2016).	10
Figure 2. Schematic configuration of sampling zones for the FEBEX-DP project	10
Figure 3. Schematic diagram of sampling locations of the shotcrete plug (C-C-32-6) for the FEBEX-DP dismantling section 32	11
Figure 4. Photographs of the overcoring method (left), shotcrete-bentonite overcore sample (center) and the X-ray CT image (right) focusing on the interface region.	13
Figure 5. 3D rendered volume of X-ray CT image data for sample C-C-32-6 at the shotcrete-bentonite interface region..	14
Figure 6. CT image XY slice sequence (down z axis) of FEBEX bentonite showing the craquelure or “chickenwire” patterns of cracks evolving into pores	15
Figure 7. CT image of shotcrete showing typical texture of angular grains in a fine-grained matrix.....	16
Figure 8. Schematic diagram of sampling locations for FEBEX-DP dismantling sections.....	20
Figure 9. BSEI with Ca element profile line scan retrieved from X-ray map of the shotcrete-bentonite interface region	21
Figure 10. Sample set BM-D-49-(1,2,3) in close contact with perforated steel mesh liner surrounding heater assembly.	21
Figure 11. Micro-XRF energy spectrum of elements detected in the shotcrete-bentonite thin section sample.....	22
Figure 12. Micro-XRF maps for Ca and S at the shotcrete-bentonite interface.....	22
Figure 13. Plot of relative humidity (RH) vs. X_{hs} for bentonite hydration in URL experiments and model predictions for Na, K, Ca, and Mg smectite.....	23
Figure 14. Diagrammatic picture of the closure test drift (CTD) at the Mizunami URL site, Japan.....	23

Acronym List

BRIE	Bentonite Rock Interaction Experiment
CIEMAT	Centro de Investigaciones Energéticas, Medioambientales y Tecnológicas
CT	Micro Computerized Tomography
CTD	Closure Test Drift
DECOVALEX	DEvelopment of COupled models and their VALIDation against EXperiments
DOE	Department of Energy
DOE-NE	DOE Office of Nuclear Energy
DR	Disposal Research
EBS	Engineered Barrier System
EDS	Energy Dispersive Spectroscopy
EMPA	Electron Microprobe Analysis
FCRD	Fuel Cycle Research and Development
FCT	Fuel Cycle Technologies
FEBEX-DP	Full-scale Engineering Barrier Experiments – Dismantling Project
FEPs	Features, Events and Processes
GTS	Grimsel Test Site
HLW	High Level Waste
JAEA	Japan Atomic Energy Agency
PA	Performance Assessment
QA	Quality Assurance
R&D	Research & Development
SEM	Scanning Electron Microscopy
SKB	Swedish Nuclear Fuel and Waste Management Company
SNL	Sandia National Laboratories
UFD	Used Fuel Disposition
UFDC	Used Fuel Disposition Campaign
UNF	Used Nuclear Fuel
URL	Underground Research Laboratory
XRF	X-ray Fluorescence

I. Introduction

The Used Fuel Disposition Campaign (UFDC) within the DOE Fuel Cycle Technologies (FCT) program has been engaging in international collaborations between repository R&D programs for high-level waste (HLW) disposal to leverage on gathered knowledge and laboratory/field data of near- and far-field processes from experiments at underground research laboratories (URL). Heater test experiments at URLs provide a unique opportunity to mimetically study the thermal effects of heat-generating nuclear waste in subsurface repository environments. Various configurations of these experiments have been carried out at various URLs according to the disposal design concepts of the hosting country repository program. The FEBEX (Full-scale Engineered Barrier Experiment in Crystalline Host Rock) project is a large-scale heater test experiment originated by the Spanish radioactive waste management agency (Empresa Nacional de Residuos Radiactivos S.A. – ENRESA) at the Grimsel Test Site (GTS) URL in Switzerland. The project was subsequently managed by CIEMAT. FEBEX-DP is a concerted effort of various international partners working on the evaluation of sensor data and characterization of samples obtained during the course of this field test and subsequent dismantling. The main purpose of these field-scale experiments is to evaluate feasibility for creation of an engineered barrier system (EBS) with a horizontal configuration according to the Spanish concept of deep geological disposal of high-level radioactive waste in crystalline rock. Another key aspect of this project is to improve the knowledge of coupled processes such as thermal-hydro-mechanical (THM) and thermal-hydro-chemical (THC) operating in the near-field environment. The focus of these is on model development and validation of predictions through model implementation in computational tools to simulate coupled THM and THC processes.

The current phase of FEBEX-DP focuses on the dismantling of heater #2 (see Fig. 1) conducted during 2015 with the goal of disassembling all the remaining sections of the FEBEX “in situ test” after 18+ year of heating and sensor/probe data (García-Siñeriz et al., 2016; Martinez et al., 2016). This dismantling activity involves sampling of barrier bentonite, steel liner, sensors, embedded metallic components (e.g., metal coupons), and near-field sections with tracer components. Given the time length for this field experiment, it provides a unique opportunity to conduct research and evaluate the fate of barrier components under repository conditions. It should be noted that a previous partial dismantling of FEBEX heater #1 was conducted after 5 years while heater #2 continued operating without disruption. Details regarding the FEBEX-DP project can be found at the GTS website <http://www.grimsel.com/gts-phase-v/febex/febex-i-introduction->.

The main goal of this report section is to document preliminary sample characterization results using X-ray CT (micro computerized tomography) imaging, SEM/EDS analyses, and micro-X-ray fluorescence (XRF) of samples obtained from FEBEX-DP phase of heater #2 which include: 1) overcore sample from the shotcrete plug – bentonite interface, and samples from sections 49 and 58 (see Fig. 2) corresponding to spatial domains near and far from the heater zone, respectively. Other activities such as the newly-started DECOVALEX-19 (Task C) and ongoing clay hydration model comparisons with data from SKB (Task 8) BRIE dismantling of bentonite parcels will be discussed briefly. The shotcrete – bentonite sample is far from the heater zone as well. The analyzed samples in this report only pertain to the shotcrete – bentonite overcore and samples from section 49 sampled close or in contact with the steel liner mesh surrounding the heating element. Samples obtained at a distance from the steel liner in section 49 and those from section 58 will be analyzed at a later time. SEM/EDS analyses were conducted in both shotcrete – bentonite overcore thin sections and granular samples from section 49 whereas the X-ray CT image analysis was only performed on epoxied overcore samples. The main objective of this characterization study is to (1) identify spatial heterogeneities of barrier materials near and far from EBS interfaces that can inform process models (e.g., porous media transport), and (2) analyze the extent of chemical variations and heterogeneities

(e.g., reaction fronts) at EBS interfaces and bulk barrier materials. The FEBEX bentonite is composed of 93% smectite with 2% quartz, 3% plagioclase, and 2% cristobalite plus minor accessory phases such as calcite and K-feldspar (Huertas et al., 2000; Missana and García-Gutiérrez, 2007).

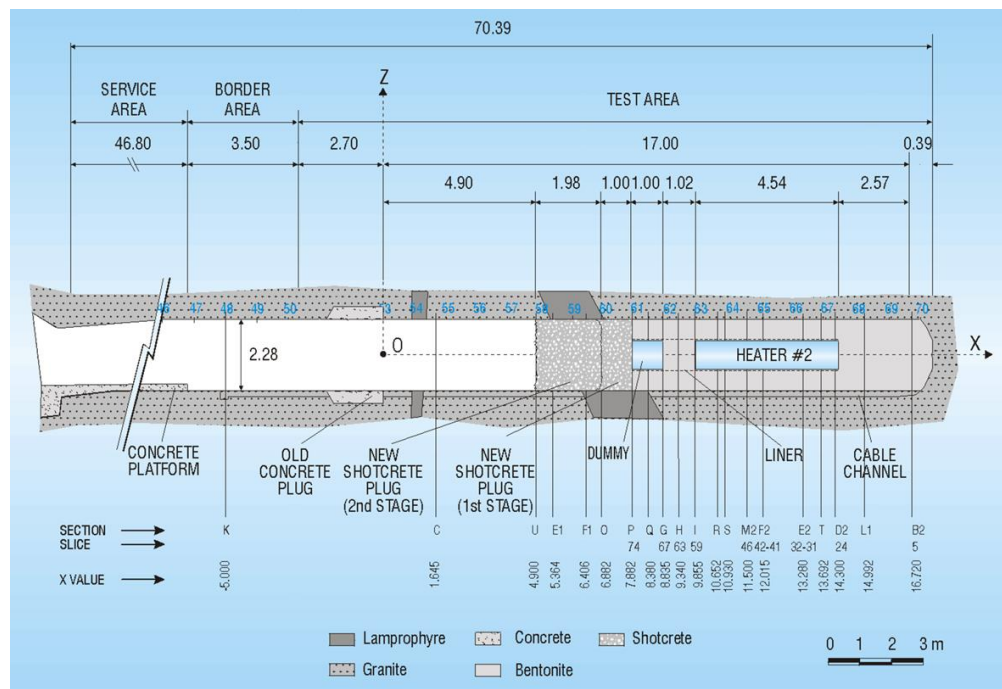


Figure 1. Schematic layout of the FEBEX "in-situ" field test after the first partial dismantling showing the configuration of heater #2 at the GTS URL (García-Siñeriz et al., 2016).

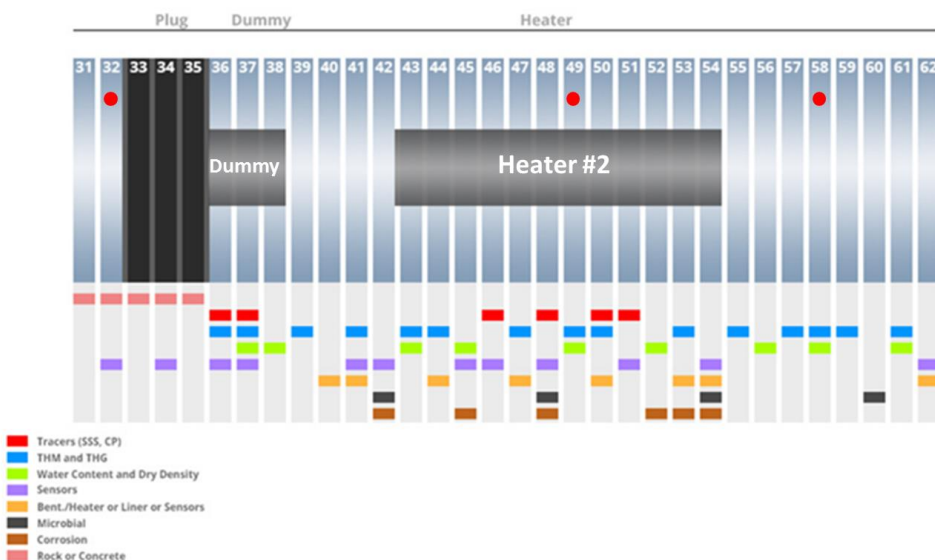


Figure 2. Schematic configuration of sampling zones (indicated by vertical light blue bars) for the FEBEX-DP project. Filled red circles indicate zones for samples obtained by Sandia National Laboratories (SNL). Source: FEBEX-DP website (members area): <http://www.grimsel.com/gts-phase-vi/febex-dp/febex-dp-introduction>.

II. X-Ray CT Imaging of FEBEX-DP Samples: Shotcrete-Bentonite Interface

The application X-ray CT imaging is well suited for core samples due to its non-destructive nature, excellent scanning resolution (e.g., 10 microns), the ability to analyze relatively large specimens (in the order of cm in length), and the generation of 2D-3D digital image data for textural evaluation. The overall friability of compacted bentonite clay makes the retrieval of intact core samples very difficult. The shotcrete-bentonite overcore sample is ideal for performing X-ray CT image analysis since the overcoring technique provides for an epoxied core with well-preserved integrity and presumably minimal damage during retrieval. Figure 3 shows the location for sample C-C-32-6 overcore (section 32) used in this characterization study.

Although the integrity of the sample in hand specimen is remarkable, some minor cracks are visible particularly along the interface between the epoxy and bentonite clay. Still, the state retrieved core sample is very good and makes it ideal for obtaining thin sections for optical microscopy and X-ray CT imaging. Polished thin sections made for optical microscopy show textural features like the extensive occurrence of cracks in the bentonite matrix and circular pores with a wide range of sizes in shotcrete. However, optical evaluation of mineral phases in thin section was difficult due to poor optics. Moreover, thin section polishing could have introduced artifacts such as removal of bentonite clay or smearing due to the “softness” and expansive nature of clay material.

The X-ray CT imaging setup used in this study is a North Star Imaging Inc. X50 system. It utilizes a Comet 225kV constant potential X-ray Source in conjunction with a Varian 2520V flat panel detector. North Star Imaging Inc. software was utilized for 3D reconstruction and to create 2D slices of the 3D volume rendering. The 2D image slices were subsequently used as input for further image post-processing using North Star Imaging Inc. software and the open source ImageJ/Fiji software package (<http://imagej.net/Fiji>; <http://fiji.sc/>). The scanning resolution is 10.5 microns in a helical step scan mode. This scanning resolution was deemed sufficient to resolve textural features down to the sub-millimeter scale and it is focused on the shotcrete-bentonite interface region.

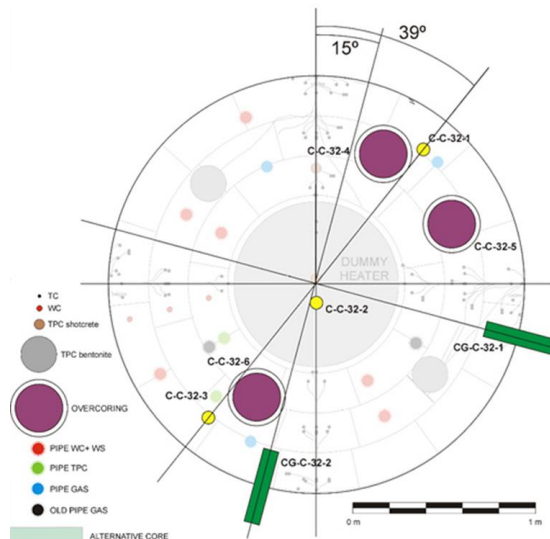


Figure 3. Schematic diagram of sampling locations of the shotcrete plug (C-C-32-6) for the FEBEX-DP dismantling section 32. See Fig. 2 for section location. (source: FEBEX-DP website (members area): <http://www.grimsel.com/gts-phase-vi/febex-dp/febex-dp-introduction.>)

The current stage of the X-ray CT imaging study (Fig. 4) of the overcored sample focused on the interface region as shown in Fig. 4. The salient features from the analysis of 2D slices is the common occurrence of microcracks in bentonite and pores (no cracks) in shotcrete. Formation of gaping cracks and pores in bentonite tends to form near or at the shotcrete-bentonite interface whereas in other cases these are found at the interface of dissimilar materials (bentonite-epoxy). Crack formation is not only restricted to areas close to material interfaces but are also common to bulk bentonite regions as well. The cracks seen in the Figures 5 a-c have nominal apertures ranging from a few hundred microns up to about a millimeter for large cracks. Most crack apertures fall within the micron/sub-millimeter scale range. The 3D projection of the CT scan slice stacks shows the extent and connectivity of cracks in the bentonite phase. Connected crack lengths can extend to length distances exceeding 1000 microns, in some cases in some cases evolving to or terminating into large pores. There is no discernable preferred orientation for cracks at the scale of these analyses. However, typical crack pattern characteristics resembles that of a “tree” branch network with smaller-aperture cracks forking from a larger-aperture branch. Further analyses of 2D-3D image stacks show these “tree” branch networks evolving into craquelure or “chickenwire” patterns in many cases connected by rectilinear and jagged segments (see Figure 6 a-c). The bentonite also has minor embedded granular material from which cracks that either radiate towards the clay matrix or surrounds the grains. It should be noted that the rather heterogeneous nature of microcrack distribution also give rise to localized regions without pores or crack features at interfaces and the bulk bentonite. This is indicative of apparent localized “sealed” regions at the interface.

The shotcrete texture tends to be more regular with granular material embedded in a fine-grained matrix with dark spots interpreted as round-shape pores/voids having a wide size range (Fig. 7). The shapes and sizes of these pores/voids plus the apparent lack of secondary solid precipitation suggests these are the result of entrapped air during the shotcrete emplacement. No microcracks at the scale of those observed in bentonite were resolved in shotcrete, even at the interfaces of large pores or grains. 3D pore/void connectivity still needs to be assessed from the digital image analysis. However, a preliminary assessment of the extent of void connectivity in shotcrete suggests these are often isolated except when localized at the shotcrete-bentonite interface.

The origin of microcracks in bentonite as observed in the shotcrete-bentonite core can be difficult to assess given the number of potential mechanisms in the creation of such features. For instance, sampling artifacts during overcore retrieval or desiccation and shrinkage due to *in situ* or *ex situ* drying conditions could induce crack formation in bentonite. It should be noted the overcoreing technique employed in obtaining this sample is remarkable in preserving core material in the least disturbed state. Regardless of the origin of cracks, which in many cases is based on subjective criteria by the observer’s evaluation, a description of microcrack patterns in bentonite is still very valuable in advancing common traits to similar structures observed in other environments. For example, desiccation cracks on clay surfaces or commonly known as “mud cracks” as a result of dehydration and shrinkage have been studied for decades motivated by the performance of clay-bearing geotechnical covers/liners and its importance to soil management (Corte and Higashi, 1964; Gebrenegus et al., 2011; Kulander et al., 1990; Morris et al., 1992).

CT imaging methodologies have been applied to studies of bentonite clay mixtures that have undergone drying/shrinkage to examine structural features such as desiccation crack morphology and dynamics under various conditions (DeCarlo and Shokri, 2014; Gebrenegus et al., 2011; Gebrenegus et al., 2006; Tuller et al., 2013). The overall morphological features observed in the current analysis and the CT imaging study of Gebrenegus et al. (2011) in sand-bentonite mixtures share some remarkable similarities, particularly the craquelure pattern and other microcrack network characteristics. Their study assessed the evolution of 3D networks of desiccation cracks in sand-

bentonite mixture under controlled conditions of temperature, pore solution chemistry, and bentonite content (Gebrenegus et al., 2011). They concluded that crack porosities (or pore volume fraction occupied by cracks) increased with bentonite content for samples exposed to drying. This is consistent with the occurrence of these features in the samples considering that FEBEX bentonite content is about 92% smectite clay. However, Gebrenegus et al. (2011) observed a decrease in hydraulic conductivity with increasing bentonite content. These authors also ascribe drying rates as an important factor in controlling crack porosities whereas pore solution chemistry has less influence.

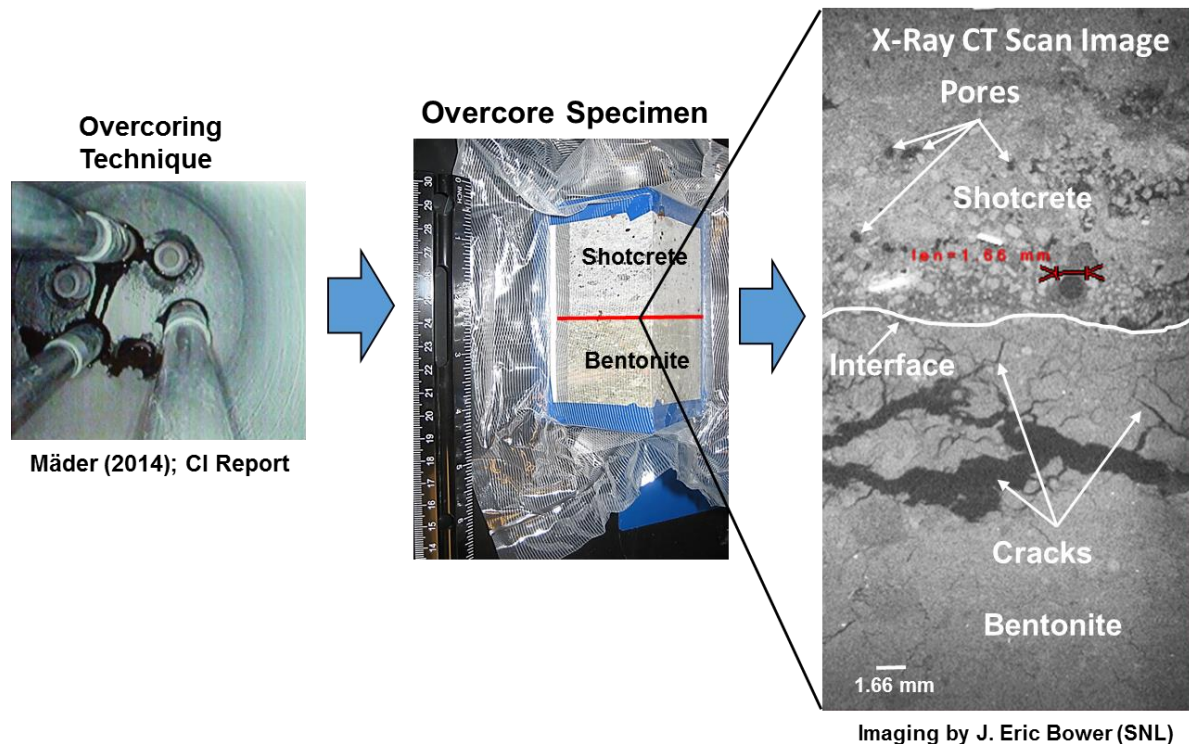


Figure 4. Photographs of the overcoring method (left), shotcrete-bentonite overcore sample (center) and the X-ray CT image (right) focusing on the interface region.

The occurrence and distribution of these microcracks in bentonite due to drying/shrinkage is key to evaluating clay barrier performance given its strong influence to moisture transport, clay swelling, and therefore permeability/porosity properties of the barrier. This is particularly important in the assessment of barrier performance during dry/wet cycles as anticipated for HLW upon emplacement in disposal galleries. Some key aspects of CT imaging studies are the quantification of crack apertures and porosities based on 3D image treatment algorithms and corrections to eliminate noise and other artifacts. This operation is necessary to attain the required resolution of crack networks and perform segmentation thresholding to resolve features of interest. Currently, image smoothing and thresholding tools in the ImageJ-Fiji software package seem adequate to qualitatively resolve major 2D-3D morphological features and patterns. However, automatic segmentation and quantification of crack apertures can be a quite involved process given the complexity of recognizing and separating phases of interest with the obtained resolution plus the huge demand on computational resources in handling massive amounts of data. These techniques will be explored with continuation of the CT imaging work in FY17 on FEBEX-DP samples at locations adjacent and far from the heater.

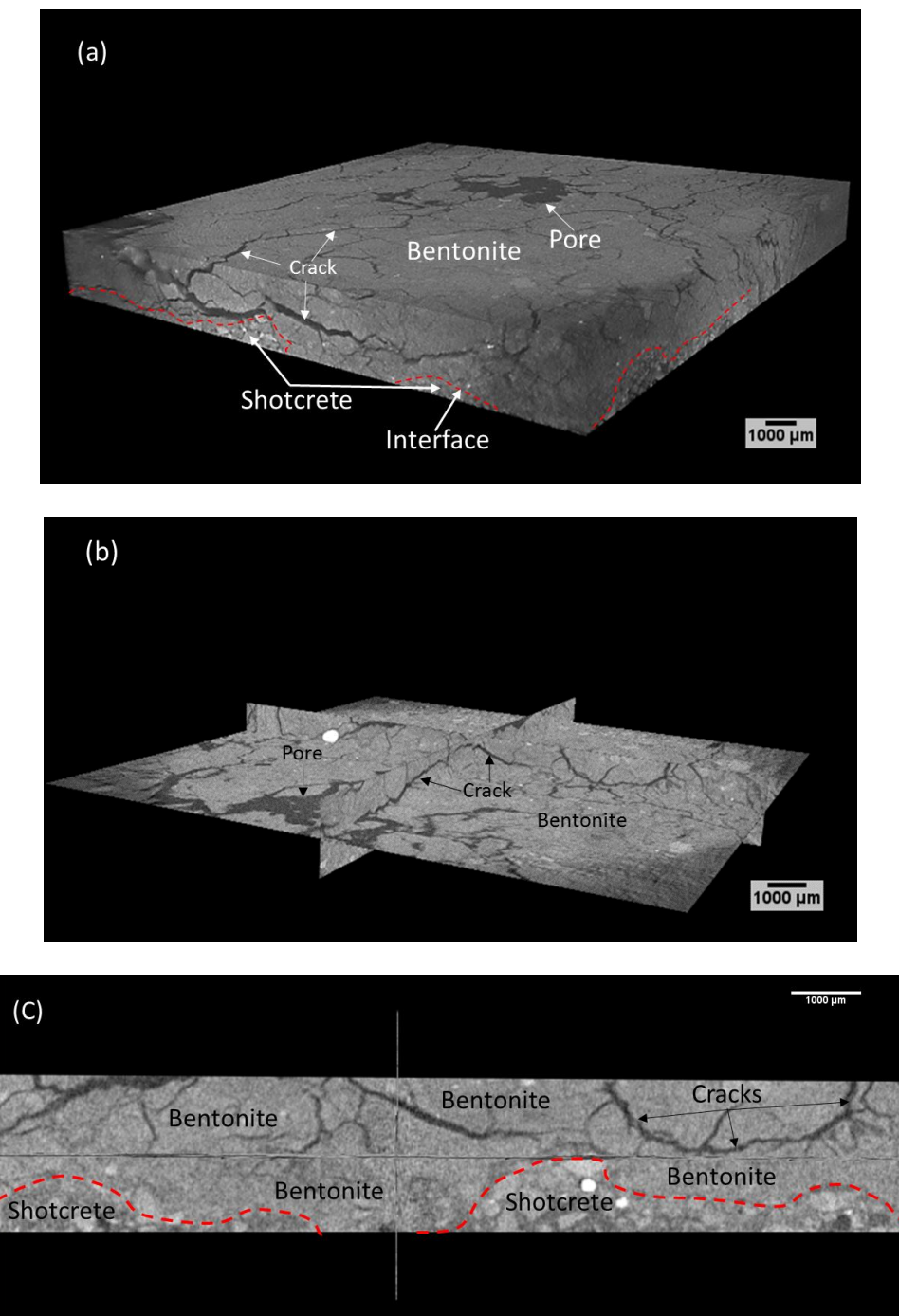


Figure 5. (a) 3D rendered volume of X-ray CT image data for sample C-C-32-6 at the shotcrete-bentonite interface (red dashed line) region. Notice the 3D crack network connectivity to other cracks and large pores in the bentonite region; (b) orthoslice projection of the volume in (a) with the horizontal plane near the shotcrete-bentonite interface; (c) 2D orthoslice (plan view) projection of the shotcrete-bentonite interface (red dashed line) showing its irregular nature. The length of the rectangular front face in (c) is ~1.3 cm.

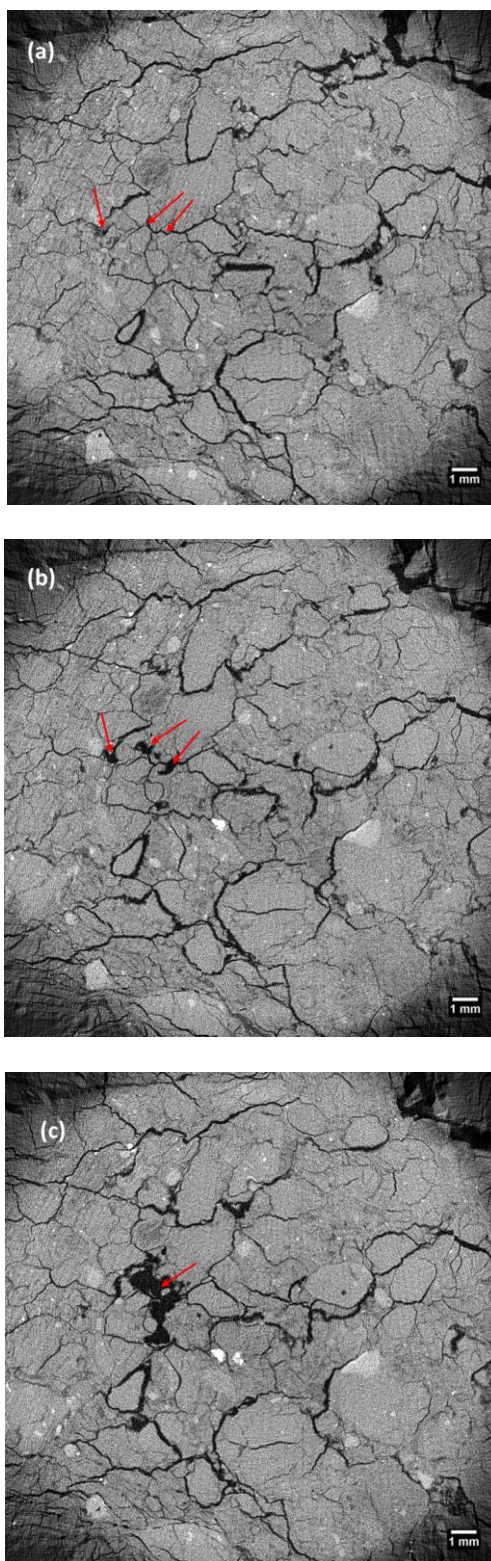


Figure 6. CT image XY slice sequence (down z axis) of FEBEX bentonite showing the craquelure or “chickenwire” patterns of cracks evolving into pores. Red arrows in panels a-c delineate: (a) cracks, (b) small pores, and (c) large pores.

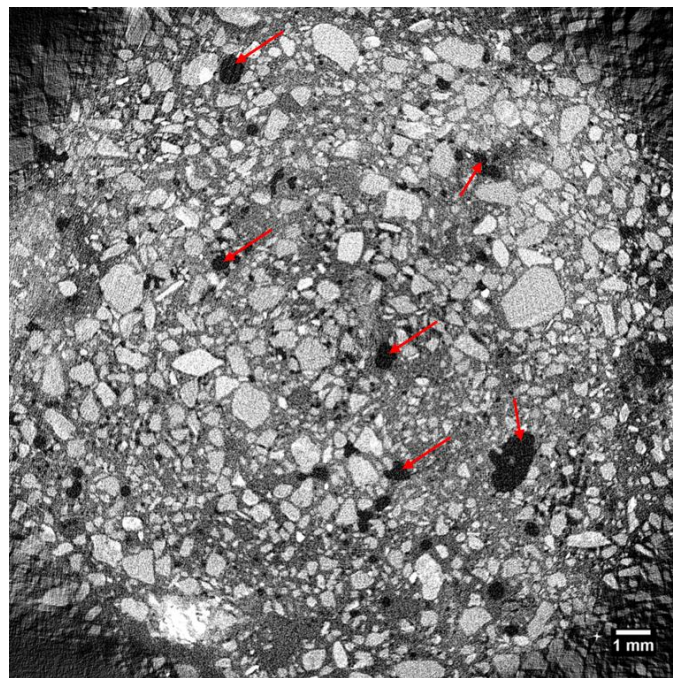


Figure 7. CT image of shotcrete showing typical texture of angular grains in a fine-grained matrix. Dark spots marked by the red arrows are interpreted as pore spaces based on preliminary evaluation of digital image stacks.

III. SEM/EDS and Micro-XRF Analysis of FEBEX-DP Samples

The effects of porosity enhancement and reduction (i.e., clogging) in barrier materials and interfaces due to mineral dissolution and precipitation has been a topic of investigation particularly in their assessment in reactive-transport models (Marty et al., 2015; Xie et al., 2015). The manifestation of this process as interactions of shotcrete with clay rock where clogging/sealing has been observed as a result of cement carbonation (Gaboreau et al., 2012). However, these “clogged” zones have been described by the authors as heterogeneous along the interface and with varying levels of mineralogical alteration. With this in mind, SEM/EDS (or electron microprobe analysis – EMPA) is an excellent technique to conduct spatial characterization of compositional heterogeneities at the shotcrete-bentonite interface and granular separates through X-ray elemental mapping, line scans, and spot analyses. Although the overall compositional characterization of solids is possible with SEM/EDS, unequivocal identification of many phases is not possible at this time. Such an analysis would require the combined use of techniques such as high resolution transmission electron microscopy (HRTEM), EDS, and X-ray diffraction (XRD). The use of HRTEM and XRD characterization methods will be explored in the future. Figure 8(a,b) shows sample locations for Sections 49 and 58 considered in this characterization study.

SEM/EDS analyses were performed using a TESCAN (Warrendale, PA) Vega 3 LMU tungsten filament scanning electron microscope (SEM) operated at 30 kV accelerating voltage. Back-scattered electron imaging (BSEI) was conducted under low vacuum mode and micrographs were collected using an annular YAG scintillator backscatter electron detector. EDS analyses were

obtained using an EDAX® Element fixed working distance silicon drift detector with a 25 mm² sensor.

The SEM/EDS analysis of the shotcrete-bentonite interface were conducted on polished thin sections from the overcore sample whereas samples from Section 49 (BM-D-49-1,2,3) close to the heater (Fig. 8b) were analyzed as uncoated grain mounts. Samples from Section 58 were not analyzed at this time but this is planned for FY17 work.

Fig. 8 shows a BSEI micrograph and an EDS line scan of Ca across the shotcrete-bentonite interface. Similar to the CT image, the BSEI analysis show the granular texture of shotcrete with angular grains having a fairly wide size range embedded in a fine-grained matrix. The bentonite region shows cracks resembling the craquelure pattern observed in the CT imaging analysis along with some minor accessory grains. The purpose of the line scan and X-ray maps is to probe for elemental distributions indicative of a reactive front or mineral phase alteration along the interface region.

Ca is a ubiquitous component in many of both FEBEX bentonite and shotcrete phases and its overall distribution should serve as an indicator of alteration at the interface as shown in Fig. 8. The peak Ca counts observed along the line scan transect (Fig. 9) are for a grain which is presumably portlandite based on the detection of elevated Ca and O only in X-ray maps. Based on various EDS X-ray maps and line scans, there is no indication of pervasive alteration or mineralization in the analyzed interface regions. Notice that on both sides of the Ca peak in Fig. 9, elemental counts decreased to nominal levels that are comparable to both sides of the interface. This indicates little or low levels of alteration within the interface region. Other elemental profiles also show a similar behavior across the shotcrete-bentonite interface. Likewise, analysis of textures using BSEI and EDS at the micron level also indicates little or no alteration along the interface.

BSEI/EDS analyses were conducted samples from Section 49 (samples BM-D-49-1,2,3) close to the steel mesh surrounding the heater. These samples were in contact with the corroded carbon steel mesh as indicated by the rusty-colored circular rind on bentonite (Figs. 10 a,b). EDS elemental analyses of bentonite sampled from this rind show mainly clay with low K content and a few grains with enriched regions in Fe (Figs 10c-e). Although there seems to be some correlation between K and Fe based on X-ray maps (Figs. 10c,d), these results are still preliminary and more analyses are needed to further evaluate such correlation or whether these are Fe-rich coatings or just Fe-bearing clay. Overall, EDS spot analyses of these samples indicate levels of K at detectable levels whereas Fe tends to be more localized on certain regions. Phase identification using XRD on these rusty-colored samples is planned for FY17.

Compositional analysis using micro – X-ray Fluorescence (XRF) was conducted on the same polished thin section sample described above for SEM/BSEI/EDS analyses (Fig. 10). Micro-XRF allows for micron-scale compositional analysis but covering a larger scan area. The micro-XRF analysis was performed using a Bruker M4 Tornado micro-XRF mapping system. The instrument was equipped with a micro-focused Rh source (50 kV, 600 μ A) with a poly-capillary optic (~30 μ m spot-size). The detector system employed a silicon-drift detector to collect fluorescence spectra from the specimen. The specimen was secured to the x-y translation stage within the M4 chamber, and XRF spectra were collected under vacuum conditions (~10⁻³ Torr). The XRF-mapping dataset for the thin-section specimen was collected as a large datacube with full X-ray spectra (4096 channels, 0 to 40 keV range) collected at each pixel in a 2D array. The step-size employed for the micro-XRF spatial map was 50 μ m. This resulted in a 502 \times 860 matrix for the map which covered an area ~24 \times ~35 mm², thus incorporating the entire cross-sectioned specimen. Total data collection time was ~90 minutes. The dimensionally of the datacube (502 \times 860 \times 4096) was greater than 1.7 billion elements, and encompassed a file size of 747 MB. Elemental maps for individual atomic species

were generated within the M4 software package. Micro-XRF maps were generated for the elements Ca, Al, Si, K, Fe, S, Cl, Cu, Mn, Pd, Zn, Zr, and Ti.

Fig. 11 shows the energy spectrum of elements detected in the sample for which maps were generated. Fig. 12 shows micro-XRF maps for Ca and S indicating slight or virtually no alteration in the bentonite side. This observation is consistent with the SEM/EDS X-ray map analyses described previously. These Ca and S compositional maps in Fig. 12 also suggest the existence of an apparent millimeter-scale depletion zone in shotcrete close to the interface. The depletion zone is demarcated by some gradation from the bulk shotcrete towards the bentonite interface which is depicted by the Ca map. The depletion zone doesn't appear to traverse the bentonite side suggesting a reaction zone confined mainly to the shotcrete side. However, this observation is very preliminary and more micro-XRF maps are needed to assess spatial compositional heterogeneities of shotcrete in the bulk.

All these observations regarding the spatial extent of reaction between shotcrete and bentonite are consistent with those of other investigators in the FEBEX-DP project (Turrero et al., 2016) working with similar samples. The use of micro-XRF has the advantage of minimal sample preparation and scanning sample areas from mm^2 to cm^2 at a high spatial resolution for a wide range of elements. This technique is more flexible and better suited for the specimen sizes collected from the dismantling phase activities where other microscopic techniques (e.g., SEM/EDS), although useful, would otherwise be much more laborious. Extending the application of micro-XRF to samples from core locations away from the interface (i.e., bulk) are planned for FY17.

IV. SKB Bentonite Rock Interaction Experiment (BRIE): Clay Hydration Modeling

The Bentonite Rock Interaction Experiment (BRIE) at the Äspö Hard Rock Laboratory has provided valuable data within the goals of: (1) obtaining an improved understanding of water exchange across the bentonite-rock interface, (2) water flow in rock matrix and fractures, and (3) enhance our understanding of bentonite wetting towards the development of predictive models of porous clay barrier materials. Clay hydration thermodynamic modeling of end-member compositions has already been described in Jové Colón et al. (2013) based on a sub-regular Margules-type solid solution formulation. Its implementation into the microporosity model by Sedighi and Thomas (2014) is described in Birkholzer et al. (2015). The results of this model representation are in overall agreement with the clay hydration data for bentonite backfill barrier materials considered in EBS repository concepts (Fig. 13). The main conclusion is that smectite clay type and composition will strongly influence swelling behavior during hydration. For example, clay hydration trends between monovalent and divalent cationic smectite compositions in bentonite will be different as exemplified in Fig. 13. FEBEX bentonite is predominantly Ca-bearing whereas MX80 is predominantly Na-bearing with other components (e.g., Ca and K) in their chemical compositions. This is illustrated by the predicted end-member trends and bentonite hydration data in Fig. 13.

Although the predicted end-member clay hydration profiles are in overall agreement with data trends, smectite in these bentonites do not have end-member compositions. From Fig. 13, one could deduce that non-end-member clay compositions, properly extrapolated between end-member bounds, would result in better agreement with the data. Extrapolation between end-members treated as a simple mixture of two phases can have the advantage of easing model implementation but not without caveats. Such a compositional extrapolation would be difficult to reconcile on the basis of clay structural chemistry and the thermodynamic treatment used to represent clay hydration. Mixed-layered smectite clays found in bentonites are often a mixture of different phases (e.g., smectite-illite) plus the presence of accessory minerals (quartz, feldspar). Moreover, the level of scatter and hence uncertainty in the bentonite hydration data doesn't warrant a more detailed model representation except to denote major differences in predicted trends. Even with this limitation, a more robust model representation of clay hydration paths within the framework of a microporosity model can still be advanced to predict compositionally-dependent clay swelling properties and thus molar volumes as a function of relative humidity (RH). This topic will be further investigated in FY17.

V. DECOVALEX-2019 Task C: GREET (Groundwater REcovery Experiment in Tunnel), Mizunami URL, Japan

The DECOVALEX-2019 project phase started this year with seven tasks (A-G) targeting various THMC issues based on experimental and URL field data. The Disposal in Argillite work package has expressed interest in the GREET (Groundwater REcovery Experiment in Tunnel, Mizunami URL, JAEA, Japan) URL project on the hydrochemical characterization of the site as part of the groundwater recovery activity from the closure test drift (CTD). The CTD is a tunnel section (46.5 m long \times 5.0 m wide \times 4.5 m high) of the URL sealed by plug and filled with groundwater (Fig. 14). A series of boreholes allow for monitoring water pressure and chemistry during the experiment. The goals of the GREET project as defined by the JAEA website are

(<http://www.jaea.go.jp/04/tono/miu/dataset/greet/greet.html>):

- “To understand the recovery process and mechanism of geological environment during facility closure.
- To verify the HMCB simulation methodology for recovery process in fractured granite.
- To develop the monitoring technique for facility closure phase and the appropriate closure method taking recovery process into account.”

The focus of GREET within the DECOVALEX-2019 project is to “develop the simulation procedure and technique to estimate the post closure environments in fractured media (asymmetric media)”. Within this focus, an initial will the evaluation of groundwater chemistry data currently available to assess quality and trends by conducting speciation calculations using geochemical code tools and databases. The possibility of using a reactive-transport code like PFLOTRAN will be considered to evaluate high pH waters and interactions with cementitious materials. The GREET project task leader has kindly provided access to geochemical and hydrological data to be reviewed by the participants which has stimulated good communications exchanges. A closer evaluation of the groundwater chemistry will be performed in the remainder of FY16 and during FY17.

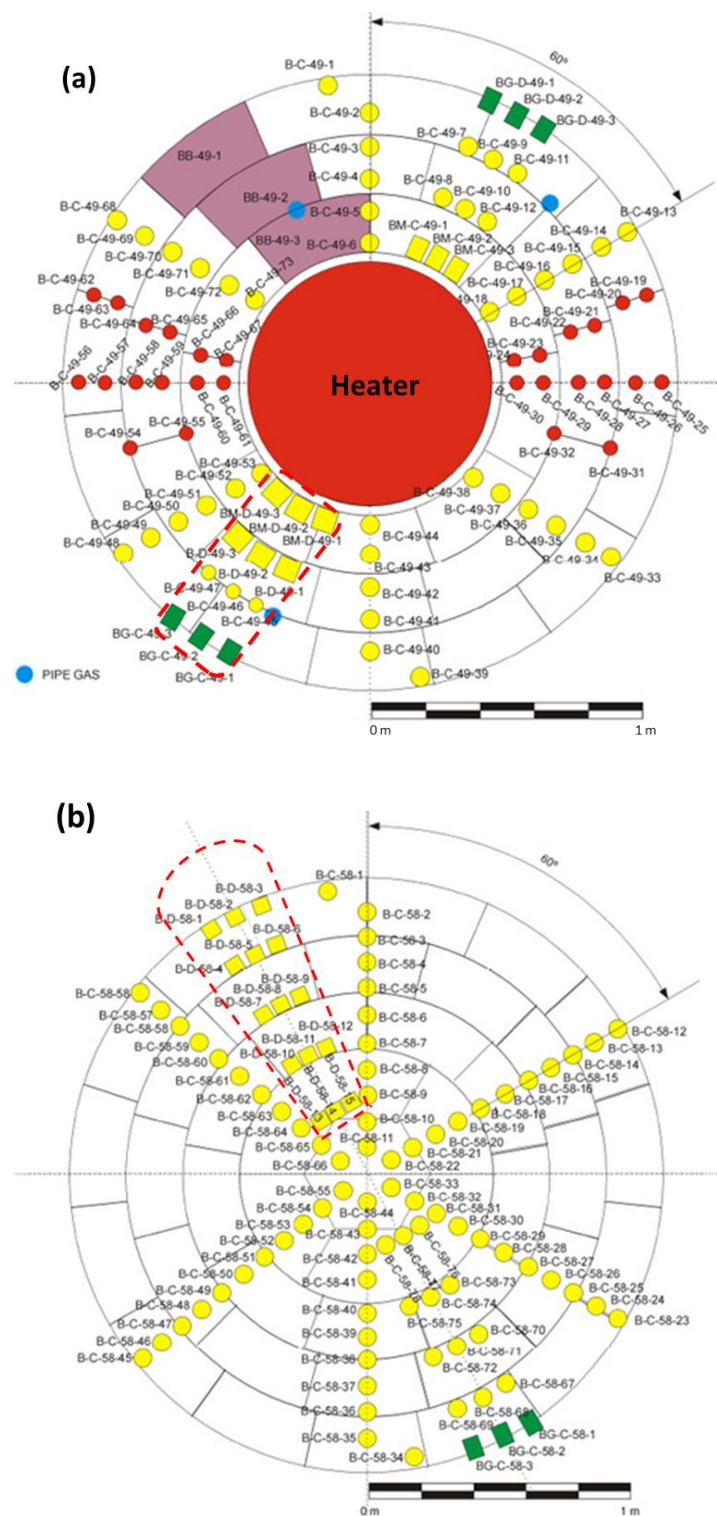


Figure 8. Schematic diagram of sampling locations for FEBEX-DP dismantling sections: (a) Section 49 adjacent to the heater; (b) Section 58 farther from the heater. The red dashed-line delineates the sample sets obtained by SNL. See Fig. 2 for section locations. (source: FEBEX-DP website (members area): <http://www.grimsel.com/gts-phase-vi/febex-dp/febex-dp-introduction.>)

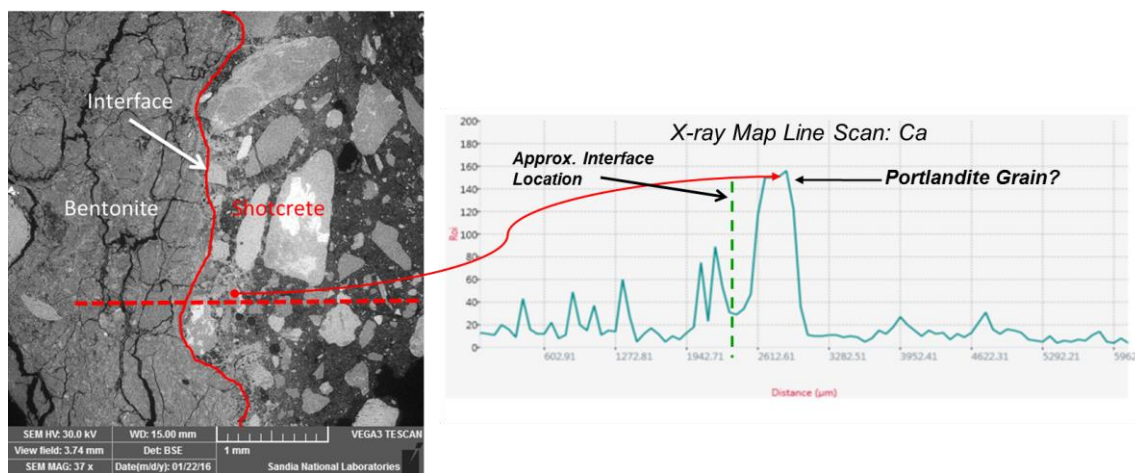


Figure 9. BSEI with Ca element profile line scan retrieved from X-ray map of the shotcrete-bentonite interface region. The horizontal red dashed-line in the BSEI is an approximate position of the line scan.

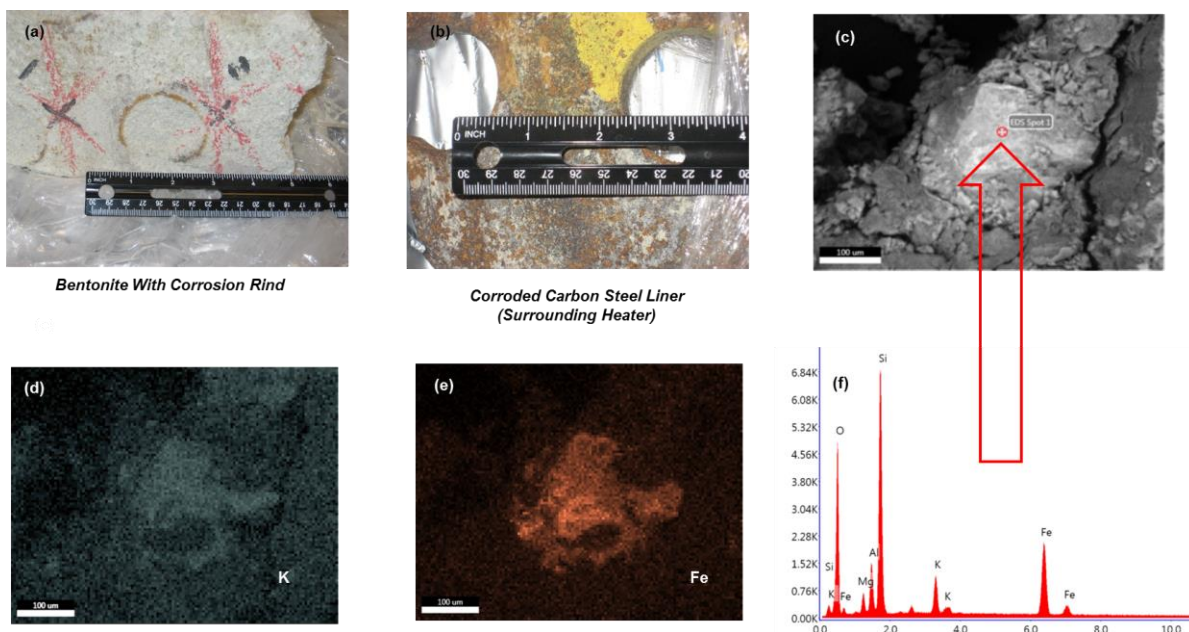


Figure 10. Sample set BM-D-49-(1,2,3) in close contact with perforated steel mesh liner surrounding heater assembly – see Fig. 8 for sample location; (a) rusty-colored corrosion rind delineating the region in contact with steel perforation; (b) corroded carbon steel mesh liner with perforations; (c) BSEI micrograph of bentonite grain sampled from corrosion rind; (d) and (e) EDS X-ray map for K and Fe, respectively, of region shown in (c); EDS spectrum of spot analysis on grain denoted by the red dot-cross symbol in (c) marked by red arrow.

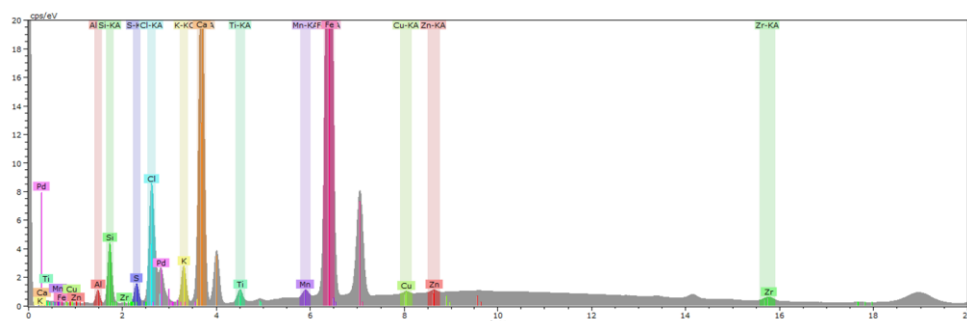


Figure 11. Micro-XRF energy spectrum of elements detected in the shotcrete-bentonite thin section sample.

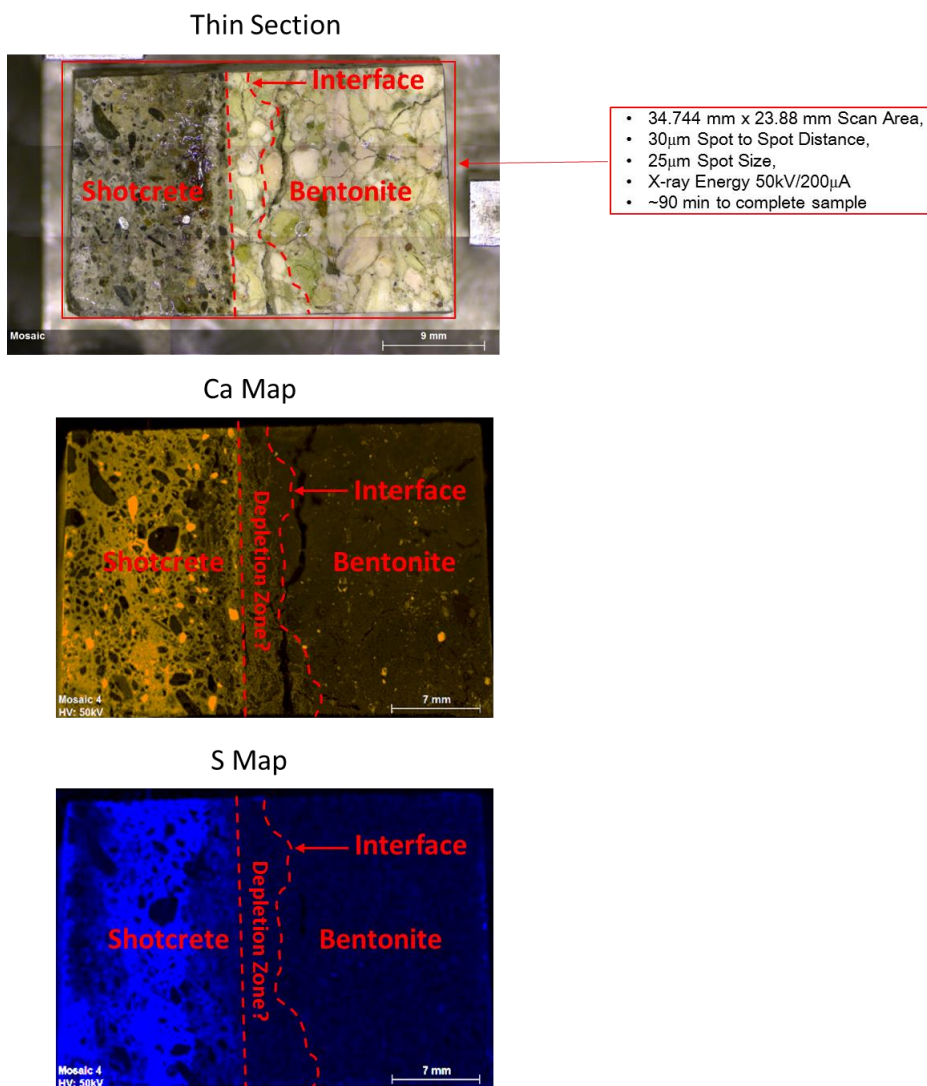


Figure 12. Micro-XRF maps for Ca and S at the shotcrete-bentonite interface. An apparent depletion zone close to the shotcrete-bentonite interface is delineated by red-dashed lines.

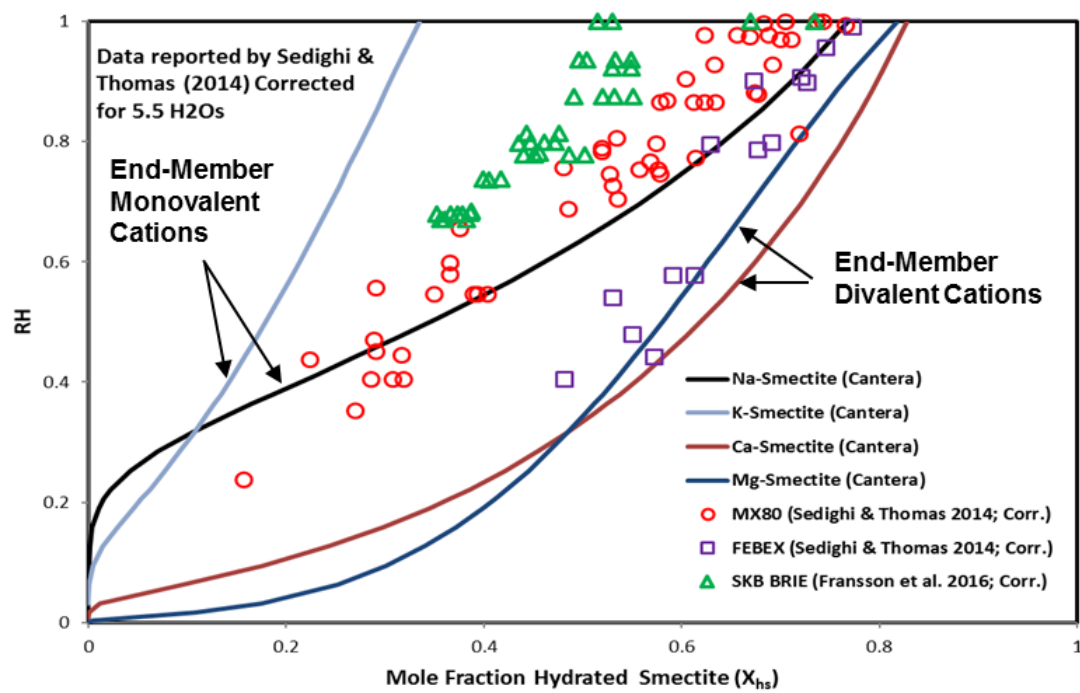


Figure 13. Plot of relative humidity (RH) vs. X_{hs} for bentonite hydration in URL experiments and model predictions for Na, K, Ca, and Mg smectite – modified after Jové Colón et al. (2013).

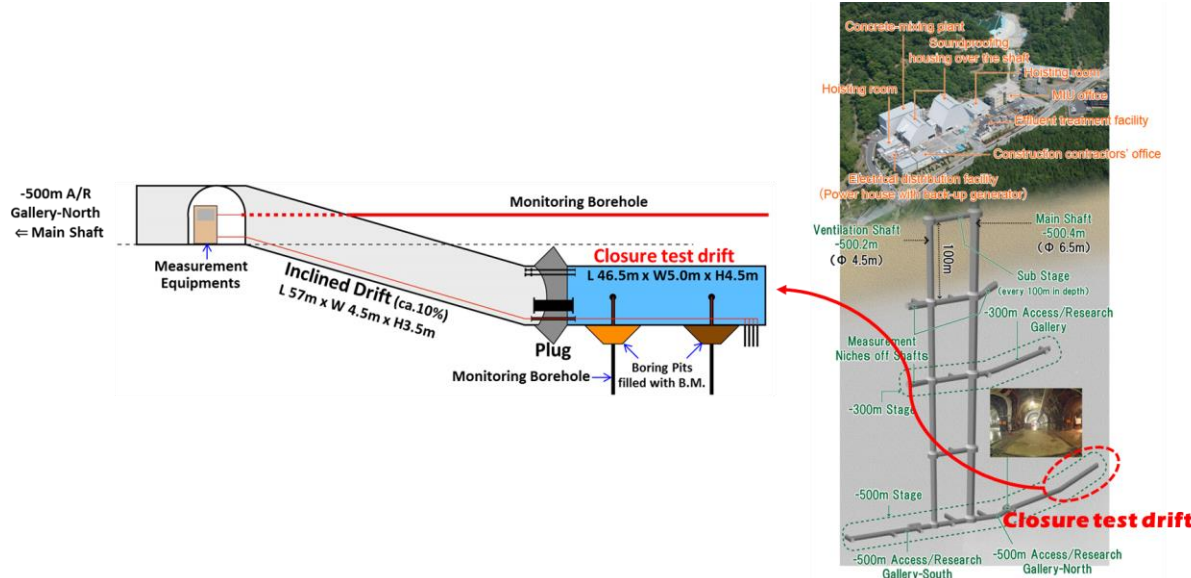


Figure 14. Diagrammatic picture of the closure test drift (CTD) at the Mizunami URL site, Japan.

V. Conclusions

- X-ray CT imaging is a powerful characterization tool in the analysis micron-to-millimeter scale structures in bentonite and shotcrete. This technique allows for the 2D-3D characterization of microcracks in FEBEX-DP shotcrete-bentonite overcore highlighting the importance of desiccation/shrinkage processes in bentonite and the nature of pores/voids in shotcrete. These observations have implications to the state of bentonite barrier material under drying conditions that could strongly influence moisture transport, clay hydration, and seal performance.
- SEMBSEI/EDS and micro-XRF characterization of the FEBEX-DP bentonite-shotcrete overcore samples revealed that much of the reaction in this region appears to be confined to the shotcrete phase and little or no alteration was experienced by bentonite. This has implications to processes such as pore clogging and secondary mineralization at interfaces considered in reactive-transport models to assess barrier performance for interactions with cement.
- SKB BRIE (Task 8): Comparisons between the clay hydration microporosity model implementation and BRIE data from post-mortem analysis of dismantled parcels show good overall correspondence with two types of bentonites. Clay hydration paths due to compositional dependencies of the smectite component can be represented by the model end-member profiles. Extension of the model to non-end-member smectite compositions will be explored in FY17.
- DECOVALEX-2019 Task C GREET Experiment: Planned work includes geochemical speciation of groundwater chemistries to evaluate data quality and the effects of interactions with cementitious materials and/or rock.

VI. FY17 Work

Planned work on **FEBEX-DP** samples for FY16 (and the remainder of FY16) will encompass the following:

- Continue CT imaging, SEM/EDS, and micro-XRF studies on samples from Section 49. Extend these analyses to samples from Section 58 located far from the heater region.
- Further expansion of the CT digital image data processing for the retrieval and quantification of geometric features of cracks and void structures.
- Conduct X-ray diffraction (XRD) analyses on selected samples at locations relative to the backfilled drift center and drift wall.
- Conduct characterization studies on bentonite samples close to the wall-rock and if possible at the bentonite/wall-rock interface.

Work on the **DECOVALEX-2019** task C will be on the evaluation of groundwater chemistry data from the GREET experiment at the Mizunami URL site in Japan. This data evaluation will initially comprise geochemical speciation of selected water chemistries using code tools and databases used in the UFD program. As part of the **SKB (Task 8)**, geochemical modeling activities will also explore expansion of the clay hydration and microporosity model to non-end-member smectite compositions.

VII. References

Birkholzer, J., Zheng, L., Reimus, P., Viswanathan, H. and Jove Colon, C.F., 2015. International Collaboration Activities in Different Geologic Disposal Environments (FCRD-UFD-2015-000079), Lawrence Berkeley National Laboratory (LBNL-1000877), Berkeley, CA USA.

Corte, A. and Higashi, A., 1964. Experimental research on desiccation cracks in soil, U.S. Army Cold Regions Research and Engineering Laboratory, CRREL-RR-66 Final Report, Alexandria, VA.

DeCarlo, K.F. and Shokri, N., 2014. Salinity effects on cracking morphology and dynamics in 3-D desiccating clays. *Water Resources Research*, 50(4): 3052-3072.

Gaboreau, S., Lerouge, C., Dewonck, S., Linard, Y., Bourbon, X., Fialips, C.I., Mazurier, A., Pret, D., Borschneck, D., Montouillout, V., Gaucher, E.C. and Claret, F., 2012. In-Situ Interaction of Cement Paste and Shotcrete with Claystones in a Deep Disposal Context. *American Journal of Science*, 312(3): 314-356.

García-Siñeriz, J.L., Abós, H., Martínez, V., De la Rosa, C., Mäder, U. and Kober, F., 2016. FEBEX DP: Dismantling of heater 2 at the FEBEX "in situ" test: Description of operations - Arbeitsbericht NAB 16-11, National Cooperative for the Disposal of Radioactive Waste (NAGRA), Wettingen, Switzerland.

Gebrenegus, T., Ghezzehei, T.A. and Tuller, M., 2011. Physicochemical controls on initiation and evolution of desiccation cracks in sand-bentonite mixtures: X-ray CT imaging and stochastic modeling. *Journal of contaminant hydrology*, 126(1): 100-112.

Gebrenegus, T., Tuller, M. and Muhunthan, B., 2006. The Application of X-ray Computed Tomography for Characterization of Surface Crack Networks in Bentonite-Sand Mixtures, *Advances in X-ray tomography for geomaterials*. ISTE Ltd. London, UK, pp. 207-212.

Huertas, F., Fuentes-Cantillana, J.L., Jullien, F., Rivas, P., Linares, J., Fariña, P., Ghoreychi, M., Jockwer, N., Kickmaier, W., Martínez, M.A., Samper, J., Alonso, E. and Elorza, F.J., 2000. Full-scale engineered barriers experiment for a deep geological repository for high-level radioactive waste in crystalline host rock (FEBEX project): Final report. EUR 19147, European Commission, Brussels.

Jové Colón, C.F., Greathouse, J.A., Teich-McGoldrick, S., Cygan, R.T., Weck, P.F., Hansen, G.A., Criscenti, L.J., Caporuscio, F.A., Cheshire, M., Rearick, M.S., McCarney, M.K., Greenberg, H.R., Wolery, T.J., Sutton, M., Zavarin, M., Kersting, A.B., Begg, J.B., Blink, J.A., Buscheck, T., Benedicto-Cordoba, A., Zhao, P., Rutqvist, J., Steefel, C.I., Birkholzer, J., Liu, H.-H., Davis, J.A., Tinnacher, R., Bourg, I., Zheng, L. and Vilarrasa, V., 2013. EBS Model Development and Evaluation Report (FCRD-UFD-2013-000312). Sandia National Laboratories, SAND2013-8512 P, Albuquerque, NM, pp. 508.

Kulander, B.R., Dean, S.L. and Ward, B.J., 1990. Fractured core analysis: interpretation, logging, and use of natural and induced fractures in core, AAPG Methods in Exploration No. 8. Published by the American Association of Petroleum Geologists (AAPG Datapages).

Martinez, V., Abós, H. and García-Siñeriz, J.L., 2016. FEBEXe: Final Sensor Data Report (FEBEX "in situ" Experiment) - Arbeitsbericht NAB 16-19, National Cooperative for the Disposal of Radioactive Waste (NAGRA), Wettingen, Switzerland.

Marty, N.C.M., Bildstein, O., Blanc, P., Claret, F., Cochebin, B., Gaucher, E.C., Jacques, D., Lartigue, J.E., Liu, S.H., Mayer, K.U., Meeussen, J.C.L., Munier, I., Pointeau, I., Su, D.Y. and Steefel, C.I., 2015.

Benchmarks for multicomponent reactive transport across a cement/clay interface. Computational Geosciences, 19(3): 635-653.

Missana, T. and García-Gutiérrez, M., 2007. Adsorption of bivalent ions (Ca (II), Sr (II) and Co (II)) onto FEBEX bentonite. Physics and Chemistry of the Earth, Parts A/B/C, 32(8): 559-567.

Morris, P.H., Graham, J. and Williams, D.J., 1992. Cracking in drying soils. Canadian Geotechnical Journal, 29(2): 263-277.

Sedighi, M. and Thomas, H.R., 2014. Micro porosity evolution in compacted swelling clays—A chemical approach. Applied Clay Science, 101: 608-618.

Tuller, M., Kulkarni, R. and Fink, W., 2013. Segmentation of X-ray CT data of porous materials: A review of global and locally adaptive algorithms. Soil–Water–Root Processes: Advances in Tomography and Imaging: 157-182.

Turrero, M.J., Torres, E., Garralon, A., Sanchez, L., Alonso, M.C., Garcia Calvo, J.L., Laguna, V.F., Cuevas, J., Ruiz, A.L., Fernandez, R., Ortega, A. and Gonzalez, D., 2016. Shotcrete and Shotcrete/Bentonite Analysis, FEBEX-DP Partner Meeting, May 3rd-4th, 2016, Kartause Ittingen, Switzerland.

Xie, M.L., Mayer, K.U., Claret, F., Alt-Epping, P., Jacques, D., Steefel, C., Chiaberge, C. and Simunek, J., 2015. Implementation and evaluation of permeability-porosity and tortuosity-porosity relationships linked to mineral dissolution-precipitation. Computational Geosciences, 19(3): 655-671.